Solution Structure of Carnobacteriocin B2 and Implications for Structure−Activity Relationships among Type IIa Bacteriocins from Lactic Acid Bacteria[†,‡]

Yunjun Wang,[§] Matthias E. Henz,[||] Nancy L. Fregeau Gallagher,[||] Shengyong Chai,[||] Alan C. Gibbs,[§] Liang Z. Yan,[||] Michael E. Stiles,[⊥] David S. Wishart,*[,§] and John C. Vederas*[,||]

Faculty of Pharmacy and Pharmaceutical Sciences and Departments of Chemistry and Agricultural, Food and Nutritional Science, University of Alberta, Edmonton, Alberta, Canada T6G 2G2

Received June 14, 1999; Revised Manuscript Received August 27, 1999

ABSTRACT: Carnobacteriocin B2 (CbnB2), a type IIa bacteriocin, is a 48 residue antimicrobial peptide from the lactic acid bacterium *Carnobacterium pisicola* LV17B. Type IIa bacteriocins have a conserved YGNGVXC sequence near the N-terminus and usually contain a disulfide bridge. CbnB2 seemed to be unique in that its two cysteines (Cys9 and Cys14) could be isolated as free thiols [Quadri et al. (1994) *J. Biol. Chem. 26*, 12204−12211]. To establish the structural consequences of the presence or absence of a disulfide bridge and to investigate if the YGNGVXC sequence is a receptor-binding motif [Fleury et al. (1996) *J. Biol. Chem. 271*, 14421−14429], the three-dimensional solution structure of CbnB2 was determined by two-dimensional ^{1}H nuclear magnetic resonance (NMR) techniques. Mass spectroscopic and thiol modification experiments on CbnB2 and on model peptides, in conjunction with activity measurements, were used to verify the redox status of CbnB2. The results show that CbnB2 readily forms a disulfide bond and that this peptide has full antimicrobial activity. NMR results indicate that CbnB2 in trifluoroethanol (TFE) has a well-defined central helical structure (residues 18−39) but a disordered N terminus. Comparison of the CbnB2 structure with the refined solution structure of leucocin A (LeuA), another type IIa bacteriocin, indicates that the central helical structure is conserved between the two peptides despite differences in sequence but that the N-terminal structure (a proposed receptor binding site) is not. This is unexpected because LeuA and CbnB2 exhibit >66% sequence identity in the first 24 residues. This suggests that the N-terminus, which had been proposed [Fleury et al. (1996) *J. Biol. Chem. 271*, 14421-14429] to be a receptor binding site of type IIa bacteriocins, may not be directly involved and that recognition of the amphiphilic helical portion is the critical feature.

Over the past two decades, dozens of antimicrobial peptides from a wide variety of plants, mammals, and microorganisms have been identified, isolated, and characterized (*3*−*5*). Many of them are lethal to bacteria, fungi, and even viruses (*6*). Interestingly, the majority of these compounds display little toxicity toward normal mammalian cells. Because of their unusual specificity, it has been proposed that such substances could eventually provide a viable alternative to conventional antibiotics, many of which are being rendered ineffective due to the emergence of new and dangerously resistant bacterial strains (*7*, *8*). An important class of ribosomally synthesized antimicrobial peptides are bacteriocins (*9*) from lactic acid bacteria (LAB), which have exhibited considerable potential as nontoxic preservatives in the food and feed industry (*10*−*12*) and may be important for the efficacy of LAB as probiotics in human and animal health (*13*).

LAB bacteriocins have been classified into four different classes (types I−IV) (*14*), of which type II bacteriocins are heat-stable peptides (typically 37−59 amino acid residues) exhibiting both cationic and hydrophobic character, whose antimicrobial activity appears to be related to their ability to disrupt cytoplasmic membranes of target bacterial cells. Carnobacteriocin B2 (CbnB2) was isolated from the culture supernatant of *Carnobacterium piscicola* LV17B (*1*, *15*, *16*). It is a type IIa bacteriocin, which is characterized by the

[†] Financial support was provided by the Natural Sciences and Engineering Research Council of Canada, the Protein Engineering Network of Centres of Excellence, Bristol Myers-Squibb (Canada), and the Alberta Heritage Foundation for Medical Research. Y.W. was supported by a Pharmaceutical Manufacturer's Association of Canada−Medical Research Council (PMAC−MRC) postgraduate scholarship. M.E.H. was supported by a Swiss National Science Foundation postdoctoral fellowship.

[‡] The coordinate files for carnobacteriocin B2 and the refined leucocin A structure have been deposited in the Brookhaven Protein Data Bank (filenames 1CW5 and 1CW6, respectively).

* Address correspondence to this author. J.C.V.: Tel 780-492-5475; FAX 780-492-8231; e-mail john.vederas@ualberta.ca. D.S.W.: FAX 780-492-1217; e-mail DSW@REDPOLL.PHARMACY.UALBERTA.CA.

[§] Faculty of Pharmacy and Pharmaceutical Sciences.

[||] Department of Chemistry.

[⊥] Department of Agricultural, Food and Nutritional Science.

[1] Abbreviations: CbnB2, carnobacteriocin B2; DCM, dichloromethane; DMF, dimethylformamide; DMSO, dimethyl sulfoxide; DQF-COSY, double-quantum-filtered correlation spectroscopy; DSS, 2,2-dimethyl-2-silapentane-5-sulfonic acid; DTT, dithiothreitol; ES-MS, electrospray mass spectrometry; FMOC, 9-fluorenylmethyloxycarbonyl; HBTU, *O*-benzotriazole-*N*,*N*,*N*′,*N*′-tetramethyluronium hexafluorophosphate; HPLC, high-performance liquid chromatography; LAB, lactic acid bacteria; LeuA, leucocin A; NMM, *N*-methylmorpholine; NMR, nuclear magnetic resonance; NOE, nuclear Overhauser effect; NOESY, two-dimensional nuclear Overhauser effect spectroscopy; RMS, root-mean-square; TFA, trifluoroacetic acid; TFE, trifluoroethanol; TOCSY, total correlation spectroscopy.

10.1021/bi991351x CCC: $18.00
Published on Web 11/05/1999

Bacteriocin	Mature Sequence
Leu A	KYYGNGVHCTKSGCSVNWGEA----FS----AGVHRLANGGNGFW
Mesentericin	KYYGNGVHCTKSGCSVNWGEA----AS----AGIHRLANGGNGFW
Cbn B2	VNYGNGVSCSKTKCSVNWGQAFQERYTAGINSFVSGVASGAGSIGRRP
Pediocin PA	KYYGNGVTCGKHSCSVDWGKA----TTCIINNGAMAWATGGHQGNHKC
Curvacin A	ARSYGNGVYCNNKKCWVNRGEATQ----SIIGGMISGWASGLAGM
Sakacin P	KYYGNGVHCGKHSCTVDWGTA----IGNIGNNAAANWATGGNAGWNK

FIGURE 1: Amino acid sequences of selected type IIa bacteriocins.

conserved heptapeptide sequence Tyr-Gly-Asn-Gly-Val-Xaa-Cys near the N-terminus (Figure 1). Its spectrum of antimicrobial activity includes many LAB as well as strains of potentially pathogenic *Enterococcus* and *Listeria* species. CbnB2 is ribosomally synthesized as a 66 residue precursor peptide, precarnobacteriocin B2; posttranslational cleavage at a Gly^{-2}-Gly^{-1} site to remove an 18-amino acid leader sequence from the N-terminus then yields the fully active 48 residue bacteriocin (i.e., CbnB2) (*15, 16*).

The YGNGVXC motif of type IIa bacteriocins usually has the cysteine as part of a disulfide bridge (*5, 12*). These bacteriocins may require a unidentified membrane-bound protein receptor, and both the N-terminal motif as well as the C-terminal portion have been suggested as recognition sequences (*2, 17*). Thus far the only type II bacteriocin whose three-dimensional structure has been solved is leucocin A (LeuA), a 37 residue peptide isolated from *Leuconostoc gelidum* UAL187 (*18, 19*). NMR studies show that LeuA adopts a well-defined tertiary structure that is composed of a three-stranded antiparallel β-sheet (residues 2−16) followed by an amphiphilic α-helix (residues 17−31) in both TFE and dodecylphosphocholine (DPC) micelles (*20*). Interestingly, the same peptide is essentially unstructured in water or aqueous DMSO (*20, 21*).

Although CbnB2 has great sequence similarity to other type IIa bacteriocins near the N-terminus (Figure 1), unlike them, CbnB2 can be obtained without a disulfide bond between the two conserved cysteines, Cys9 and Cys14 (*1*). This disulfide was deemed to be critical for antimicrobial activity of mesentericin Y105 (*2*), a peptide that differs from Leu A only at positions 22 and 26. To ascertain the structural consequences and importance of the disulfide functionality in CbnB2 and to assess whether there is a common "receptor-binding" structural motif (*2, 17*), in the present study we determine the three-dimensional solution structure of CbnB2 by NMR spectroscopy. In addition, the redox chemistry of the two conserved cysteines in CbnB2 and model peptides is examined in mass spectrometry and chemical modification experiments. Comparison of the structures of LeuA and CbnB2 shows that high sequence conservation of the N-terminal region does not generate identical structural motifs, whereas the more variable sequences of the central region result in similar amphiphilic α-helices that may be involved in receptor recognition.

EXPERIMENTAL SECTION

Peptide Synthesis, Purification, and Characterization. An N-terminal fragment of CbnB2 (1−22) was synthesized at BioTools Inc. (Edmonton, AB) and purified to >95% homogeneity by reverse-phase HPLC with an acetonitrile/H_2O gradient (0.05% TFA) on a Beckman System Gold Nouveau instrument. The molecular weight of the peptide was determined by electrospray mass spectrometry (Fisons VG Trio 2000 ES-MS) as 2346.21 ± 2.63 (calculated mass 2349.6).

Six model hexapeptides were synthesized on a Rainin PS 3 peptide synthesizer by standard Fmoc solid-phase peptide chemistry (*22*). Specifically, Wang resin (0.2 mmol) was swollen in DMF, then thoroughly washed with DCM (3 × 10 mL) and DMF (5 × 10 mL). The C-terminal amino acid was activated with HBTU and NMM (1:1:2) and allowed to react with the solid support. Each amino acid was assembled in turn by automated cycles of deprotection, activation, and coupling. The amino acids were deprotected by reaction with 20% piperidine in DMF for 10 min followed by washing with DCM (3 × 10 mL) and DMF (5 × 10 mL). Each residue was activated by mixing the protected amino acid (0.8 mmol in 2.7 mL of DMF) with HBTU (0.7 mmol in DMF) and a slight excess (1.6 mmol) of neat NMM for 5 min. The activated amino acids were condensed to the peptide resin by agitation with N_2 bubbling for 45 min and then washed with DCM (3 × 10 mL) and DMF (5 × 10 mL). The N-terminal acetylation was accomplished by reacting with NMM (800 μL), acetic anhydride (500 μL), and DMF (15 μL) for 15 min. The peptide was cleaved with 10 mL of a cleavage cocktail (95% TFA 5% H_2O) for 2 h. It was then precipitated with cold ether (30 mL). The crude peptides were purified by reverse-phase HPLC on a C-18 21 × 250 mm Zorbax 300 SB column with a binary (H_2O acetonitrile) gradient at a flow rate of 8 mL/min with aqueous 0.1% TFA and 0.1% TFA in acetonitrile as the mobile phase. The eluent was monitored at 220 nm and positive fractions were analyzed by HPLC and ES-MS to confirm their identity.

Kinetic Study of the Redox Reaction on the Hexapeptides. For the kinetic study of the model hexapeptides, 1 mg of the oxidized peptide was dissolved in 280 μL of 45 mM pH 5.2 deuterated phosphate trifluoroethanol buffer. Dithiothreitol (DTT) (9.75 mg) was dissolved in 1 mL of 45 mM pH 5.2 deuterated phosphate buffer. A 50 μL portion of this solution corresponding to 3.5−11 equiv of DTT was added to the initial solution. The concentration of the peptide was determined by ^{1}H NMR peak integration of the DTT resonances (methylene protons) and selected peptide resonances (N-terminal acetyl group protons and threonine γ-protons). The reduction of each peptide was monitored by 1D and 2D ^{1}H NMR spectroscopy and the kinetics was measured by the time-dependent loss of peak intensity of resonances corresponding to β-protons of oxidized cysteine

(~3.2 ppm). After the reduction reaction was complete, the pH was adjusted to 8.0 and the solution was degassed with excess oxygen. The subsequent oxidation reaction was monitored by 1D and 2D ^{1}H NMR spectroscopy.

Production and Isolation of CbnB2. CbnB2 was prepared as previously described (*1*). Briefly, 50 mL of *Carnobacterium piscicola* LV17B preculture was inoculated into 5 L of medium containing (per liter): casamino acids (15 g), yeast extract (5 g), glucose (25 g), $K_2HO_4 \cdot 3H_2O$ (1 g), $MgSO_4$ (0.1 g), $MnSO_4 \cdot 4H_2O$ (0.05 g), and Tween 80 (1 mL). The culture was maintained at pH 6.2 by addition of 1 M NaOH (controlled by Chem-Cadet, Cole-Parmer, Chicago, IL) and gently stirred under an N_2 atmosphere for 26 h at 25 °C. After centrifugation, the culture supernatant was loaded onto a 4.5 × 50 cm Superlite DAX-8 column (Sigma−Aldrich Co.) preequilibrated with 0.1% TFA in water. The sample was eluted from the column with 0−80% (v/v) ethanol gradient (2 L of 0%, 20%, and 35%; 1.5 L of 50%; and 1 L of 80% ethanol). The 50% ethanol fraction having the most antimicrobial activity was concentrated in vacuo to about 20 mL at 30 °C. It was then mixed with an equivalent volume of acetonitrile (MeCN) and loaded onto a 5 × 25 cm Sephadex LH-60 (Sigma) column preequilibrated with 50% MeCN and 0.1% TFA in water. After elution, the bioactive fractions were pooled and concentrated to 10 mL. The final purification was accomplished by reverse-phase HPLC with a C8 Vydac column (10 × 250 mm, 10-μm particle size, 300 Å pore size) using a gradient from 20% to 31% MeCN in 0.1% TFA and a flow rate of 2.5 mL/min. Mass spectrometry of fresh CbnB2 was done by direct solution injection (50% aqueous MeCN, 0.1% TFA) using a VG Quattro triple-quadrupole instrument with an electrospray ionization source (Fisons, Manchester, U.K.). The identity of the purified CbnB2 was confirmed by mass spectrometry and coinjection on HPLC with the reference sample from the first reported isolation of CbnB2 (*1*). The molecular weight was found to be 4968.00 ± 0.49 (calcd 4969.51, average of monoisotopes for the reduced form) and varied about 1 mass unit from run to run. Coinjection on HPLC gave a single peak with the same retention time as the sample from the original isolation.

Reduction and Carboamidomethylation of CbnB2. Two identical samples were prepared by dissolving 50 μg of CbnB2 into 0.5 mL of 0.6 M Tris-HCl buffer, pH 8.6, containing 6 M guanidine hydrochloride. An aliquot of 20 μL of freshly prepared 280 mM DTT was added to one of the samples. After a brief period of vortexing, the sample was incubated at 37 °C for 30 min and then 150 μL of freshly prepared iodoacetamide (0.6 mM) was added dropwise over 2 min under an argon environment. The sample was then incubated in the absence of light for 1 h at 37 °C. The other sample was reacted with iodoacetamide under exactly the same conditions but without prior DTT reduction. The reaction mixture was directly loaded onto a reverse-phase HPLC (C8 Vydac column, 4.6 × 250 mm, 5-μm particle size, 300 Å pore size, flow rate 1 mL/min) for further purification. After concentration in vacuo, the purified product was redissolved in aqueous MeCN (50%, 0.1% TFA) for mass spectrometry. The same experiments were also done on a synthetic version of the N-terminus of CbnB2 (residues 1−22). The peptide, in which both cysteines were reduced, was dissolved in a 0.1 M ammonium bicarbonate buffer (pH 8.0) and stirred under an oxygen environment overnight. The oxidized product was purified by reverse-phase HPLC as above. Two identical samples of both oxidized and reduced forms of the 22-mer were reacted with iodoacetamide as described above, one being treated with DTT whereas the other was not. Mass spectra of those samples were collected under the same conditions as for the full-length CbnB2 samples.

NMR Sample Preparation. A total of 5.0 mg of CbnB2 was dissolved in 700 μL of TFE-d_3/H_2O (90%/10% v/v). The material was then sonicated (under dry N_2) for 1 min with a Cole-Palmer sonicator to accelerate solution. The final concentration of the peptide was 0.9 mM. The TFE-d_3 used in the sample preparation was 99.94% deuterated (Cambridge Isotope Laboratories, Andover, MA). All samples were acidified to pH 2.8 (uncorrected meter reading) by addition of TFA (0.1% final concentration).

NMR Spectroscopy. All ^{1}H NMR experiments were performed on Unity 500 or Inova 600 MHz NMR spectrometers equipped with a 5-mm triple resonance probe. TOCSY experiments were done with the basic pulse sequence proposed by Bax and Davis (*23*). Acquisition times were set to 0.2 s, relaxation delays were 2.0 s, and spin-lock (MLEV-17) mixing times were 50 ms. NOESY (*24*, *25*) data were collected essentially identically to the TOCSY data, with mixing times ranging from 150 to 300 ms. DQF-COSY spectra were also collected by standard protocols (*26*, *27*). All two-dimensional spectra were collected with 256 t_1 increments and spectral widths of 6000 Hz in both dimensions. To distinguish between overlapping signals, as well as to determine the relative amide ^{1}H exchange rates, additional TOCSY and NOESY spectra were collected at 10, 20, 25, and 30 °C (±0.1 °C), respectively. Water suppression was achieved by solvent presaturation during the relaxation delay period. Prior to Fourier transformation, the data matrix was zero-filled to 4K × 4K complex points and multiplied by an approximate 90°-shifted sine-bell squared weighting function in both dimensions. The residual signal from protonated TFE was used as a secondary chemical shift reference [3.88 ppm downfield from 2,2-dimethyl-2-silapentane-5-sulfonic acid (DSS) (*28*)].

Complete ^{1}H NMR assignments for CbnB2 were obtained by well-established procedures (*29*, *30*) (see Supporting Information). Individual spin systems were initially identified from TOCSY and COSY spectra and then sequentially assigned by use of NOESY spectra. $^3J_{HN\alpha}$ coupling constants were obtained from line-width measurements from both TOCSY and NOESY spectra (*31*). Amide proton temperature coefficients were determined by measuring amide chemical shift changes from TOCSY and NOESY spectra collected over a range of temperatures (10−35 °C).

Structure Calculations for CbnB2. Interproton distance restraints were derived by analyzing previously assigned NOE peaks present in NOESY spectra acquired with 150−200 ms mixing times. Assigned NOE intensities, measured by volume integration, were classified into four groups (strong, medium, weak, and very weak) corresponding to interproton distance restraints of 1.8−2.8 Å, 1.8−4.0 Å, 1.8−5.0 Å, and 1.8−6.0 Å respectively. $^3J_{HN\alpha}$ coupling constants measured from TOCSY and NOESY spectra by line-width measurements (*31*) yielded a total of 15 ϕ backbone torsion angles restraints. Backbone ϕ angle restraints were set to

$-120° \pm 30°$ for those residues exhibiting large coupling constants ($^3J_{HNH\alpha} > 8.5$ Hz). For those residues in the well-defined central helical region (i.e., $^3J_{HNH\alpha} < 6.0$ Hz), their ϕ torsion angles were calculated from the Karplus equation (*32*) and assigned a variance of $\pm 20°$. Backbone ψ angle restraints were obtained from an analysis of the $d_{N\alpha}/d_{\alpha N}$ ratios (*33*). For $d_{N\alpha}/d_{\alpha N}$ ratios less than 1, the ψ angle restraint was set to $120° \pm 100°$. For $d_{N\alpha}/d_{\alpha N}$ ratios greater than 1, the ψ angle restraint was set to $-30° \pm 110°$. During the calculation, all ω angles were set to $180° \pm 10°$. Backbone hydrogen bonds were identified by analyzing the NH temperature coefficients and comparing them to the previously derived secondary structure. Each hydrogen bond was defined by two distance restraints, $d_{O-H} = 1.8-2.4$ Å and $d_{O-N} = 2.7-3.5$ Å. The disulfide bond between Cys9 and Cys14 was defined by three distance restraints, $d_{S(i)-S(j)} = 2.02 \pm 0.05$ Å, $d_{S(i)-C\gamma(j)} = 2.99 \pm 0.05$ Å, and $d_{C\gamma(i)-S(j)} = 2.99 \pm 0.05$ Å. Force constants for NOE-derived distance restraints were set to 50 kcal mol^{-1} Å^{-2}. Dihedral angle force constants were initially set to 5 kcal mol^{-1} rad^{-2} during the high-temperature dynamics run and increased to 200 kcal mol^{-1} rad^{-2} during the annealing.

In total, 319 NOE distance restraints (145 intraresidue, 89 sequential, 63 medium-range, and 22 hydrogen-bond-derived restraints), 88 dihedral angle restraints (15 ϕ angle restraints, 22 ψ angle restraints, and 47 ω angle restraints), 8 $^3J_{HNH\alpha}$ coupling constant restraints, and 163 proton chemical shift restraints were used to generate our ensemble of CbnB2 structures. This represents an average of 13 restraints/residue.

During the first set of structure calculations, only NOE-derived interproton distance restraints were included as experimental input. Thirty structures were generated by a simulated annealing protocol (*34*) with 12 000 high-temperature steps (60 ps at 1000 K) followed by 6000 cooling steps (30 ps, final temperature of 100 K), as implemented in X-PLOR (version 3.8.5; *35*). Further refinement was done with the same protocol but with 6000 high-temperature steps (30 ps) and 4000 cooling steps (20 ps). Those structures having no interproton distance restraint violations greater than 0.5 Å were accepted and used as input structures for the second (torsion angle) phase of refinement. For the final stage of structural refinement, those structures exhibiting no interproton distance and torsion angle restraint violations greater than 0.5 Å and 5°, respectively, were accepted and further refined against the measured $^3J_{HNH\alpha}$ coupling constants (*36*) and proton chemical shift restraints (*37*). During this final refinement stage, 800 steps of conjugate-gradient minimization were performed. The force constants for $^3J_{HNH\alpha}$ coupling constant restraints and proton chemical shift restraints were 1.0 kcal mol^{-1} Hz^{-2} and 7.5 kcal mol^{-1} ppm^{-2}, respectively.

Structure Refinement of LeuA. To complete the structural refinement of LeuA, previously collected TOCSY and NOESY spectra (*20*) were reanalyzed. On the basis of the previously published chemical shift assignments for LeuA, $^3J_{HNH\alpha}$ coupling constants were measured (via line width measurements) and additional NOE peaks were assigned from the NOESY spectrum. The 18 structures previously generated by Fregeau et al. (*20*; PDB accession no. 2LEU) were used as initial input structures. These structures were first refined against the newly assigned interproton distance restraints by the previously described simulated annealing protocol and then further refined against $^3J_{HNH\alpha}$ coupling constants and proton chemical shifts. A total of 434 interproton distance restraints (155 intraresidue, 118 sequential, and 153 medium- and long-range NOE-derived distance restraints as well as 8 hydrogen-bond-derived distance restraints), 27 $^3J_{HNH\alpha}$ coupling constant restraints, and 136 proton chemical shift restraints (representing an average of 16 restraints/residue) were used during the refinement of LeuA. This compares to an average of 11 restraints/residue (407 distance restraints) used in generating the initial LeuA structure (*20*).

Structure Evaluation and Analysis. The quality of the final ensemble of both sets of CbnB2 and LeuA structures was assessed with the program PROCHECK-NMR version 3.4.4 (*38*). MOLMOL (*39*) was used to visualize, superimpose, and calculate root-mean-square (RMS) deviation values for all structures. Homology modeling of CbnB2 was conducted with the WHATIF on-line server (*40*; http://swift.embl-heidelberg.de). Theoretical ^{1}H chemical shifts were calculated with the program TOTAL (*41*). Dihedral angles were extracted with the program VADAR (*42*), and sequence dependent secondary structure analysis was performed with PepTool (*43*). The coordinate files for CbnB2 and the refined LeuA structure have been deposited in the Brookhaven Protein Data Bank (filenames 1CW5 and 1CW6, respectively).

RESULTS

Redox State of CbnB2. Mass spectrometric analysis of CbnB2 after its initial isolation (*1*) indicated that it was apparently unique among type IIa bacteriocins in that it did not possess a disulfide bond between the conserved cysteines. Initial NMR investigation showed that chemical shift values for residues in the N-terminal region were quite different from those of LeuA, whose sequence is quite similar but which does possess a disulfide linkage. Since such a linkage was reported to be essential for biological activity of mesentericin Y105 (*2*), and LeuA could not be easily kept in reduced (dithiol) state under aerobic conditions, the oxidation state of the two cysteines in antimicrobially active CbnB2 was reexamined in detail as a prelude to determination of its three-dimensional structure. The approaches employed kinetic study of the redox reaction of model peptides in conjunction with mass spectroscopy and thiol modification experiments.

On the basis of recent studies on *Escherichia coli* thioredoxin where a Lys−Cys interaction is reported (*44*), it seemed that Lys13 in CbnB2 may undergo a lysine−thiol interaction that could prevent facile oxidation to the disulfide bridge between Cys 9 and 14. To test this hypothesis, six hexapeptides that model the 9−14 region were synthesized, each with an acetyl group on the N-terminus and a C-terminal amide (Table 1). Two of these peptides are identical in sequence to residues 9−14 in native LeuA and CbnB2. The other four are homologous to the CbnB2 sequence and have specific substitutions to examine possible influence of charge. Kinetic studies of the reduction of the cyclic peptide in the presence of an excess of DTT showed a second-order reaction at pH 5.0. As expected, the reoxidization with a 50-fold excess of oxygen obeys first-order kinetics. The

Table 1: Redox Reaction Rates for Hexapeptide Analogues of 9−14 Region of LeuA and CbnB2

hexapeptides	K_{red}[a] ($min^{-1}\ \mu M^{-1}$)	K_{ox}[b] $\times 10^3$ ($min^{-1}\ \mu M^{-1}$)
AcCSKTKC-NH_2	0.7	3.6
AcCTKSGC-NH_2	1.1	1.0
AcCSKTGC-NH_2	0.4	3.0
AcCSGTKC-NH_2	0.5	1.3
AcCSGEKC-NH_2	0.1	1.1
AcCSKEKC-NH_2	0.3	5.1

[a] K_{red} is the reduction constant with excess DTT, pH ∼ 5.0−5.5. [b] K_{ox} is the oxidization constant with excess oxygen, pH ∼ 8.0−8.5.

measured reduction and oxidization rate constants for these model peptides are listed in Table 1 and show that the presence of an extra lysine does not significantly decrease the oxidization rate of the dithiol or increase the reduction rate of the corresponding disulfide. Hence the redox reactions for these model peptides are similar and indicate that the sequence between the two cysteine residues is unlikely to account for major differences in oxidation states of LeuA and CbnB2.

To reexamine the oxidation state of CbnB2, the identity of the purified CbnB2 was confirmed by mass spectrometry and coinjection on HPLC with a reference sample of CbnB2 obtained from the original isolation (*1*). The molecular weight was 4968.00 ± 0.49 (calcd 4969.51 for monoisotopic reduced form) and varied up to 1 unit from run to run due to machine calibration error. Coinjection on HPLC gave a single peak with the same retention time as an original sample. Thus, both CbnB2 samples appeared to be oxidized (i.e., possessed a disulfide bond) and had similar biological activity within experimental error.

Reduction and Carboxamidomethylation of CbnB2. The redox status of CbnB2 was further investigated by carboxamidomethylation of the CbnB2 cysteines. The molecular weights of the reaction products clearly show that CbnB2 could not be carboxamidomethylated if the sample was not first reduced with DTT; the oxidized (disulfide) form of CbnB2 was recovered in each case. Because carboxamidomethylation only occurred when the CbnB2 sample was reduced, this clearly indicates that a disulfide bond existed between the two cysteines of CbnB2 (Cys9 and Cys14) prior to reduction for samples isolated by our current protocol. Furthermore, activity studies show that the recovered unmodified CbnB2 always maintains its antimicrobial activity, whereas the carboxamidomethylated product does not. For the oxidized synthetic 22-mer (corresponding to the N-terminus of CbnB2), the same modification patterns were observed. Specifically, the two cysteine thiol groups were carboxamidomethylated only if the sample was first reduced with DTT. For the reduced form of the 22-mer, the two cysteines could be carboxamidomethylated regardless of whether DTT was used to effect disulfide reduction.

Chemical Shift Assignment and Secondary Structure of CbnB2. Circular dichroism studies indicate that, like LeuA (*20*), CbnB2 exists primarily as a random coil in pure water and assumes a defined conformation having α-helical content with increasing TFE concentration (data not shown). A complete list of the NMR assignments, including the $^3J_{HNH\alpha}$ coupling constants and amide proton temperature coefficients for CbnB2, is given in Supporting Information. The observed medium-range ($i, i + 2$; $i, i + 3$) NOEs and strong amide proton ($i, i + 1$) NOEs and characteristically small $^3J_{HNH\alpha}$ coupling constants from Trp18 to Ser39 indicate that CbnB2 adopts a helical configuration in this region. A section of the NOESY spectrum, collected at 25 °C, corresponding to this helical segment is shown in Figure 2.

It is well-known that ^{1}H NMR chemical shifts are strongly dependent on the character and nature of protein secondary structure (*45*). In particular, it has been found that α-^{1}H chemical shifts experience an upfield shift (with respect to the random coil value) when corresponding amino acids are in a helical configuration and a comparable downfield shift when the residues are in a β-strand or extended configuration (*45*−*47, 48*). Net structural chemical shifts [the observed chemical shift minus the random-coil value (*49*)] for CbnB2's α-protons are shown in Figure 3b. The nearly continuous set of upfield α-proton chemical shifts from Trp18 to Ser39 clearly confirm the existence of an α-helix in this region. Small amide temperature coefficients (<3 ppb/°C), also observed over the same region, indicate the presence of extensive hydrogen bonding and are further suggestive of a well-defined α-helical structure.

Figure 3b also shows that the α-protons for several N-terminal residues (8−17) exhibit a slight downfield shift but one that is not significant enough to indicate any well-defined β-sheet structure. Several weak NOEs between the Val7 γCH_3 protons and the Tyr3 ring protons were also observed, but no other significant medium- or long-range NOEs could be found in the N-terminus. These data, along with the random coil-like $^3J_{HNH\alpha}$ coupling constants (∼ 7 Hz) measured throughout this region, indicate that the N-terminus of CbnB2 is essentially unstructured. It is also worth noting that no NOEs (at any temperature) could be detected between Cys 9 and Cys 14 or any other residues involved in the N-terminal disulfide bond. This paucity of NOE data made it essentially impossible to determine by NMR whether CbnB2 was, in fact, reduced or oxidized. Confirmation of the oxidation state of our NMR sample by subsequent mass spectrometry and chemical modification experiments (see above) eventually allowed a disulfide constraint to be built into our final model. Evidently the rapid motions experienced by the N-terminus lead to a time-averaged dissipation of the expected NOEs (*50*). As for CbnB2's C-terminus (residues 41−48), the absence of any medium- or long-range NOEs, the random coil-like $^3J_{HNH\alpha}$ coupling constants (∼7 Hz), and the featureless net structural α-proton chemical shifts indicate that this region, too, is largely unstructured. The lack of structure for both the N- and the C-terminus was confirmed by additional TOCSY and NOESY measurements collected over a range of temperatures (10− 35 °C). These latter results indicate that the disordered structure observed for the N-terminus of CbnB2 at 25 °C is not necessarily a function of the spectral collection conditions but rather a function of the inherent structural propensity of this region.

Three-Dimensional Structure of CbnB2. A summary of the structural statistics for the final set of CbnB2 structures is provided in Table 2. The criteria for acceptance for this final set of structures were as follows: no interproton distance restraint violation greater than 0.5 Å, no dihedral angle restraint violation greater than 5°, no RMS deviation from ideal bond lengths greater than 0.02 Å, no RMS

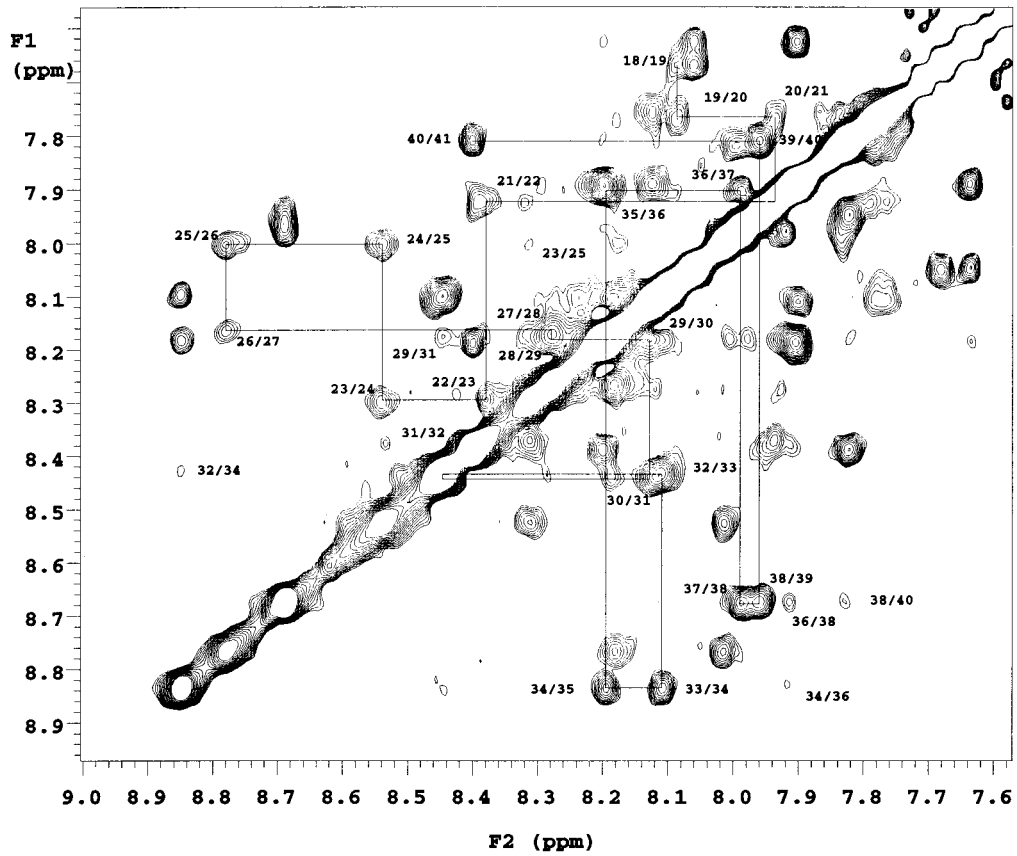

FIGURE 2: HN−HN region NOESY spectra of CbnB2. Sequential and medium-range NOE connectivities in the helical region (from Trp18 to Ser39) are indicated.

deviation from ideal bond angles greater than 2.0°, no coupling constant restraint violation greater than 1 Hz, and no more than 14 proton chemical shift restraint violations (i.e., $|\delta_{obs}-\delta_{cal}| > 0.5$ ppm) for any given structure. For some structures, several rounds of refinement were required to meet the above criteria. Twenty of the initial 30 structures eventually satisfied these criteria and were accepted into the final ensemble of CbnB2 solution structures. For the helical region (residues 19−39), the average RMS deviation relative to the mean was calculated to be 0.48 Å for the backbone atoms and 0.94 Å for all heavy atoms. Closer examination of this helix indicates that the side chains of several hydrophobic residues, Trp18, Phe22, Tyr26, Ile30, Phe33, Val34, and Val37, form a long, well-defined hydrophobic surface on one side of the helix (Figure 4). Conversely, the side chains of several hydrophilic residues, Asn17, Gln20, Glu24, Arg25, Asn31, Ser35, and Ser39, form a well-defined hydrophilic surface on the opposite side.

Refined Three-Dimensional Structure of LeuA. Because of the importance of conducting a detailed comparison between the LeuA and CbnB2 solution structures, we decided to refine the previously published LeuA structure (*20*) by taking advantage of recent advances in NMR structure refinement protocols (*36, 37*) and coupling constant measurements (*31*). During the course of this LeuA refinement, 190 new restraints were added, including 30 medium- and long-range NOE-derived distance constraints, 27 $^3J_{HN\alpha}$ coupling constant restraints, and 136 proton chemical shift restraints. The addition of these restraints improved the LeuA structure. Relative to the earlier set of LeuA structures, the RMS deviation of the backbone and heavy atoms fell from 1.10 and 1.57 Å (for the unrefined set) to just 0.67 and 1.04 Å (for the refined set). Under standard PROCHECK structure "quality" statistics, the overall *G*-factor increased from −0.7 (for the unrefined set) to just −0.1 (for the refined set). Furthermore, for the newly refined set of LeuA structures, 75% of the ϕ/ψ dihedral angles were located within the "most favorable" region of Ramachandran space, while just 65% fell into this region for the unrefined set. Equally important, the calculated chemical shifts for the N-terminal region of the refined set of LeuA structures now show substantially better agreement to the observed chemical shifts than for the unrefined set (the RMS deviation between the observed and predicted α-proton chemical shifts is 0.27 ppm for the refined set versus 0.42 ppm for the unrefined set).

Despite the evident improvement in the precision and accuracy of the LeuA structure, it is clear that the overall fold of LeuA is essentially the same as previously described (*20*). LeuA still adopts a well-defined tertiary structure from residues 2 to 31, including a three-stranded antiparallel β-sheet (residues 2−16) followed by an amphiphilic helix (residues 17−31). The β-sheet and α-helix conformation is clearly characterized by the net structural α-proton chemical shifts shown in Figure 3a.

DISCUSSION

Like other antimicrobial peptides, LAB bacteriocins are believed to disrupt membranes of target bacteria and lead to leakage of cellular contents (*5, 51*). Some, such as the lantibiotic nisin A, do not require a receptor protein in the target (*52*), but others may recognize a receptor, as yet

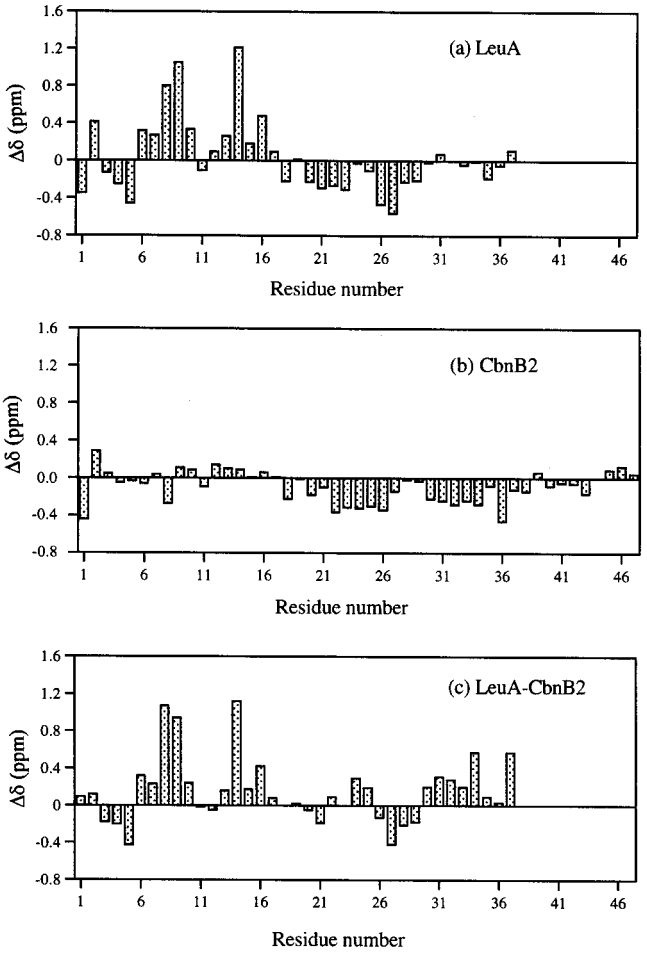

FIGURE 3: Net structural α-proton chemical shift [observed chemical shift minus the random coil chemical shift (*49*)] versus residue number for (a) CbnB2 and (b) LeuA. Panel c shows a plot of α-proton chemical shift differences between the two peptides.

Table 2: Average Atomic RMS Deviation from Mean Coordinates for CbnB2 Segments[a]

residues	backbone atoms (Å)	heavy atoms (Å)
19−39	0.48	0.94
2−18	3.51	4.61
9−14	1.14	2.18
2−7	0.99	1.91

[a] Analyzed with MOLMOL version 4.0 (see ref *39*).

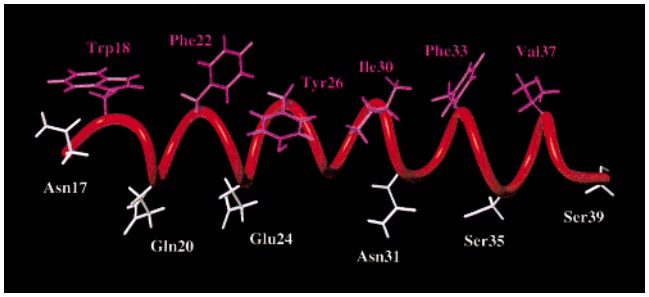

FIGURE 4: Diagram of amphipathic helical section of CbnB2.

unidentified, in the target organisms. Several lines of evidence support the existence of such a putative receptor protein for type IIa bacteriocins. There is a high level of specificity for particular target organisms among groups that are closely related. Interchange of large domains of different type IIa bacteriocins, such as pediocin, sakacin P, and curvacin A (Figure 1), give chimeric antimicrobial compounds whose specificity corresponds to the C-terminal portion (*17*). Finally, recent work shows that a peptide fragment (residues 20−34) of pediocin PA-1 *specifically* inhibits pediocin PA-1 activity, although it is not antimicrobially active and does not effectively inhibit closely related bacteriocins such as LeuA, sakacin P, and curvacin A (*51*). Although the latter studies indicate that the more sequence-variable C-terminal portion is involved in receptor recognition, other workers suggest recognition of the highly conserved N-terminal portion (*2*). It is clear that the entire peptide is essential for overall activity. For example, large fragments of these bacteriocins are inactive, and deletion of a single amino acid from the C-terminus of mesentericin Y105 drops activity by a factor of 10^5 (*2*). Detailed knowledge of the three-dimensional structure of these bacteriocins is an essential step in understanding their interactions with a protein receptor.

Most type IIa bacteriocins contain a disulfide bridge in the highly conserved N-terminal region. Although initial isolation of CbnB2 (*1*) appeared to afford the reduced bis(thiol) form of the peptide on the basis of mass spectrometric analysis, a number of subsequent isolations yielded the corresponding disulfide. Limitations of accuracy for the mass spectral methods combined with NMR spectra that showed quite different chemical shifts for the N-terminal region of CbnB2 with respect to those of highly homologous LeuA encouraged us to examine this apparent discrepancy. Synthesis of a series of hexapeptide models of the 9−14 region of CbnB2 and LeuA followed by examination of their oxidation and reduction rates (Table 1) showed that sequence variations in this portion of the bacteriocin would be unlikely to account for a dramatic difference in the propensity for disulfide bridge formation. To verify the actual oxidation state of antimicrobially active CbnB2, this compound was exposed to *N*-iodoacetamide before and after reduction. The results clearly demonstrate that the disulfide form of CbnB2 is fully active and is not modified, whereas the reduced dithiol form is converted to a bis(carboxamidomethyl) derivative that has lost all antimicrobial activity. A similar result has been reported earlier for mesentericin Y105, a 37 amino acid bacteriocin that differs from LeuA only at positions 22 and 26 in the α-helical portion (*2*). A synthetic N-terminal fragment CbnB2 1−22, was similarly modified, further confirming that the disulfide bond formation in CbnB2 proceeds very readily. Hence, dramatic differences in NMR chemical shifts in the highly homologous N-terminal regions of CbnB2 and LeuA are due to unexpected structural variations (see below).

Since the YGNGVXC sequence had been suggested to be a recognition element for a membrane-bound protein receptor (*2*), it was of interest to compare the three-dimensional structure of this region in CbnB2 and LeuA. It is clear that the CbnB2 N-terminus is highly disordered, whereas the corresponding region in LeuA forms a well-defined antiparallel β-sheet (Figure 5). The structural variance is confirmed by their α-proton chemical shift differences (Figure 3c). For CbnB2, the NOEs observed between the Val7 γCH_3 protons and the Tyr3 ring protons indicate the existence of a weak or poorly defined reverse turn in this region. The proximity of these side chains provides a small hydrophobic surface that may be important for biological

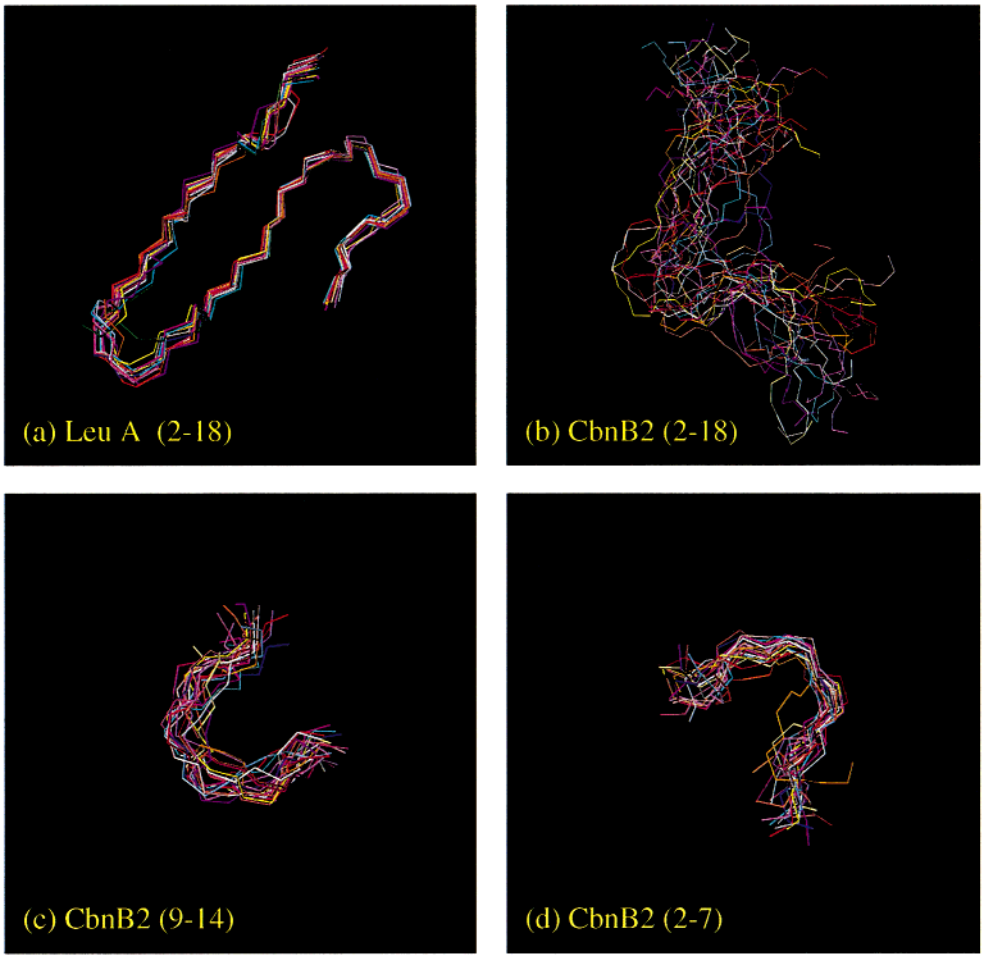

FIGURE 5: Backbone superimpositions of 20 structures of: (a) LeuA (residues 2−18), (b) CbnB2 (residues 2−18), (c) CbnB2 (residues 9−14), and (d) CbnB2 (residues 2−7).

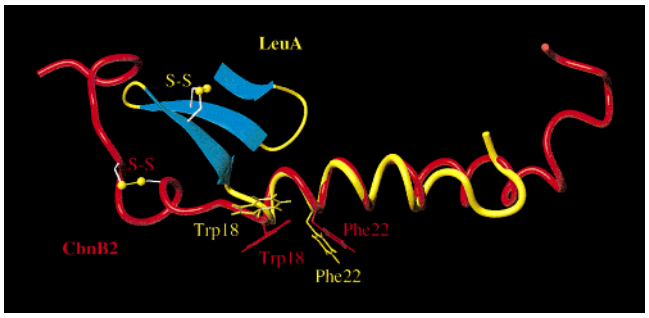

FIGURE 6: Superimposition of diagrams of CbnB2 and LeuA based on the alignment of backbone atoms from Trp18 to Phe22.

activity. In this regard, it has been shown that the substitution of Tyr3 with Phe can substantially reduce the antimicrobial activity of CbnB2 (*16*). Interestingly, both peptides share a well-defined amphipathic α-helix located near their C termini (residues 19−39 for CbnB2; residues 17−31 for LeuA) despite much greater variability in sequence (Figure 6). This result is in accord with the proposal that this region of the bacteriocin determines target specificity through binding of the putative receptor protein (*17, 51*).

To understand the possible causes for the structural differences in the N-termini of CbnB2 and LeuA, it is critical to rule out any sources of experimental error that may have led to the generation of incorrect or unreasonable structures. We investigated three possibilities: (1) differential thermal stability between LeuA and CbnB2; (2) errors in the assignments or structure of LeuA; and (3) errors in the assignments or structure of CbnB2. Differential thermal stability was examined by carefully checking the NMR data collected for CbnB2 at two lower temperatures (10 and 15 °C) and looking for evidence of additional or previously undetected structure. No significant differences in chemical shifts, coupling constants, or NOE patterns were found. This suggests that the disorder seen in the N-terminus of CbnB2 is not a consequence of thermal denaturation or low thermal stability. Similarly, we investigated whether the three-stranded β-sheet in LeuA was particularly temperature-sensitive (i.e., thermally unstable). Chemical shift and NOE measurements at 25 and 35 °C indicated that this structure in LeuA is, in fact, quite stable. These results suggest that differences in thermal stability are not the primary reason for the observed structural differences in LeuA and CbnB2.

Although the structural refinement of LeuA could be improved, it very closely resembles the previously published version (*20*), including the well-defined N-terminal three-stranded β-sheet. In light of this result, we decided to investigate the last possible source of error: incomplete structural sampling during the generation of the CbnB2 structures.

When a solution structure of a relatively flexible region of a peptide (such as the N-terminus of CbnB2) is generated, it is always possible that the structure generation protocol does not completely sample all parts of conformation space. Consequently, it may be possible that a structure in the

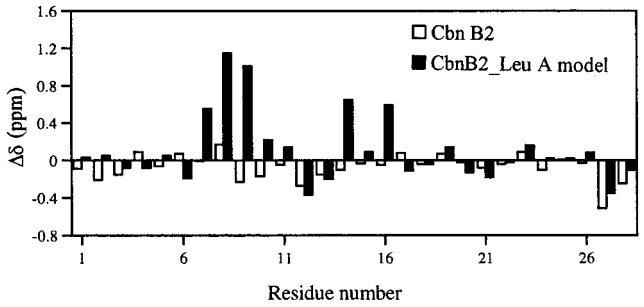

FIGURE 7: Calculated α-proton chemical shifts for the CbnB2 structural model that uses the LeuA backbone as a template and comparison to observed values.

N-terminus of CbnB2, identical to the one in LeuA, is completely compatible with the observed NMR data. To investigate this possibility we decided to "thread" (*53*) the CbnB2 sequence into the refined LeuA structure and compare the calculated NMR data for this LeuA-like structure with the observed NMR data. Specifically, model structures of the first 37 residues of CbnB2 were built (via WHATIF; *40*) with our previously refined LeuA structure as a template. The correctness of this "remodeled" CbnB2 was then evaluated by comparing its predicted ^{1}H chemical shifts with the observed values by using the program TOTAL (*41*). Recently developed chemical shift calculation methods (such as TOTAL) have made it possible to accurately (±0.25 ppm) calculate ^{1}H chemical shifts for proteins having well-resolved structures (*54*, *41*). The calculated α-proton chemical shifts together with the observed values for these "remodeled" CbnB2 structures are plotted in Figure 7. From these two figures it is clear that unrealistically large α-proton chemical shift differences (greater than two standard deviations) are predicted for residues Val7, Ser8, Cys9, Cys14, and Val16 of the "remodeled" CbnB2 structure. Likewise, significant $^3J_{HNH\alpha}$ coupling constant differences are also predicted for residues Asn5 and Lys13 in the same remodeled structure. These results indicate that a three-stranded β-sheet (such as the one found in LeuA) is structurally incompatible with the observed NMR data for CbnB2. In other words, one can rule out incomplete conformational sampling as a possible reason for the structural differences observed between LeuA and CbnB2.

Why do the N-termini of LeuA and CbnB2, which have 66% sequence identity, have different structures under identical solution conditions? Although there are examples where single amino acid substitutions in peptides and proteins have led to profound changes in function (*55*−*60*), these substitutions usually lead to complete denaturation or complete loss of activity. What is particularly interesting about the situation with LeuA and CbnB2 is that the observed structural differences at the same pH and solvent conditions do not seem to affect their strong antimicrobial activity. With probable sources of experimental error excluded, we believe that the best explanation for these structural differences must lie in the intrinsic nature of the two peptides and/or their surrounding solvent (TFE).

A close look at the β-sheet formed at the N-terminus of Leu A reveals that it is quite amphipathic. Indeed, four residues, Tyr2, His8, Thr10, and Ala 24, form a hydrophobic cluster on one side of the β-sheet, while another four residues, Lys1, Asn5, Cys9, and Cys14, form a weakly hydrophilic cluster on the other side. However, such an amphipathic β-sheet structure could not form in CbnB2 if it adopted the same fold as LeuA. This is because all four hydrophobic residues (Tyr2, His8, Thr10, and Ala24) in LeuA are replaced by hydrophilic or neutral residues (Asn2, Ser8, Ser10, and Glu24) in CbnB2. The significant hydrophobic/hydrophilic differences arising from these four key residue substitutions could account, at least in part, for the observed structural difference between LeuA and CbnB2.

Since TFE is known to stabilize amphipathic structures (*61*−*64*), this could be a contributing factor to the observed β-sheet at the N-terminus of LeuA. This also suggests that the LeuA β-sheet, which is seen in TFE and is less-well defined in DPC micelles (*20*), may be primarily an artifact of the solution (i.e., TFE) conditions. This further implies that the N-terminal structure of type IIa bacteriocins may not be central to their function. Detailed structural studies of other type IIa bacteriocins will likely be needed to resolve this issue.

CONCLUSION

Our results clearly show that, like other type IIa bacteriocins, CbnB2 can easily form a disulfide bond between Cys9 and Cys14. Furthermore, CbnB2 and LeuA, despite sharing considerable sequence similarity (66.6% for the first 24 residues), exhibit very different N-terminal structures in TFE. LeuA adopts a well-defined three-stranded antiparallel β-sheet whereas CbnB2 adopts a disordered structure. This structural difference between CbnB2 and LeuA can be attributed to a combination of differing secondary structural propensities and the differing effects of TFE on amphipathic structures. This study also indicates that while the N-terminal sequence may be important, the β-sheet structure found at the N-terminus of LeuA may not be critical to the antimicrobial functions of type IIa bacteriocins. These results agree with recent evidence that structural recognition by a putative receptor in target bacteria may involve the well-conserved central amphipathic helix whose actual sequence varies considerably in different bacteriocins.

ACKNOWLEDGMENT

We thank Albin Otter, Tom Nakashima, and Glen Bigam for helpful discussions and technical assistance with NMR experiments.

SUPPORTING INFORMATION AVAILABLE

Two tables showing ^{1}H NMR chemical shift assignments, $^3J_{HNH\alpha}$ coupling constants, and HN temperature coefficients for CbnB2 in TFE/H_2O, (90%/10% v/v) and statistics on structural calculations for CbnB2 and LeuA. This material is available free of charge via the Internet at http://pubs.acs.org.

REFERENCES

1. Quadri, L. E. N., Sailer, M., Roy, K. L., Vederas, J. C., and Stiles, M. E. (1994) *J. Biol. Chem. 269*, 12204−12211.
2. Fleury, Y., Dayem, M. A., Montagne, J. J., Chaboissseau, E., Le Caer, J. P., Nicolas, P., and Delfour, A. (1996) *J. Biol. Chem. 271*, 14421−14429.
3. Cammue, B. P. A., De Bolle, M. F. C., Schoffs, H. M. E., Terras, F. R. G., Thevissen, K., Osborn, R. W., Rees, S. B., and Broekaert, W. F. (1994) in *Antimicrobial peptides*

(Bomam, H. G., Marsh, J., and Goode, J. A., Eds.) pp 91−106, Wiley, New York.
4. Boman, H. G. (1995) *Annu. Rev. Immunol. 13*, 61−92.
5. Nissen-Meyer, J., and Nes, I. F. (1997) *Arch. Mirobiol. 167*, 67−77.
6. Jacob, L., and Zasloff, M. (1994) in *Antimicrobial Peptides* (Boman, H. G., Marsh, J., and Goode, J. A., Eds.) pp 91−106, Wiley, New York.
7. Nikaido, H. (1994) *Science 264*, 382−388.
8. Davies, J. (1994) *Science 264*, 375−381.
9. Bennik, M. H. J., Vanloo, B., Brasseur, R., Gorris, L. G. M., and Smid, E. J. (1998) *Biochim. Biophys. Acta 1373*, 47−58.
10. Vandenbergh, P. A. (1993) *FEMS Microbiol. Rev. 12*, 221−238.
11. Delves-Broughton, J., Blackburn, P., Evans, R. J., and Hugenholtz, J. (1996) *Antonie Van Leeuwenhoek 69*, 193−202.
12. Stiles, M. (1996) *Antonie van Leeuwenhoek 70*, 331−345.
13. Tannock, G. W., Ed. (1999) *Probiotics: A Critical Review*, Horizon Scientific Press, Wymondham, Norfolk, U.K.
14. Klaenhammer, T. R. (1993) *FEMS Microbiol. Rev. 12*, 39−86.
15. Quadri, L. E. N., Sailer, M., Terebiznik, M. R., Roy, K. L., Vederas, J. C., and Stiles, M. E. (1995) *J. Bacteriol. 177*, 1144−1151.
16. Quadri, L. E. N., Yan, L. Z., Stiles, M. E., and Vederas, J. C. (1997) *J. Biol. Chem. 272*, 3384−3388.
17. Fimland, G., Blingsmo, O. R., Sletten, K., Jung, G., Nes, I. F., and Nissenmeyer, J. (1996) *Appl. Environ. Microbiol. 62*, 3313−3318.
18. Hastings, J. W., Sailer, M., Johnson, K., Roy, K. L., Vederas, J. C., and Stiles, M. E. (1991) *J. Bacteriol. 173*, 7491−7500.
19. Van Belkum, M. J., and Stiles, M. E. (1995) *Appl. Environ. Microbiol. 61*, 3573−3579.
20. Fregeau, G. N. L., Sailer, M., Niemczura, W. P., Nakashima, T. T., Stiles, M. E., and Vederas, J. C. (1997) *Biochemistry 36*, 15062−15072.
21. Sailer, M., Helms, G. L., Henkel, T., Niemczura, W. P., Stiles, M. E., and Vederas, J. C. (1993) *Biochemistry 32*, 310−318.
22. Bodanszky, M. (1993) *Principles of Peptide Synthesis*, Springer-Verlag, Berlin.
23. Bax, A., and Davis, D. G. (1985) *J. Magn. Reson. 65*, 355−360.
24. Jeener, J., Meier, B. H., Bachmann, P., and Ernst, R. R. (1979) *J. Chem. Phys. 71*, 4546−4553.
25. Kumar, A. Ernst, R. R., and Wuthrich, K. (1980) *Biochem. Biophys. Res. Commun. 95*, 1−6.
26. Piantini, U., Søresen, O. W., and Ernst, R. R. (1982) *J. Am. Chem. Soc. 104*, 6800−6805.
27. Shaka, A. J., and Freeman, R. (1983) *J. Magn. Reson. 51*, 169−173.
28. Wishart, D. S., Bigam, C. G., Yao, J., Abildgaard, F., Dyson, H. J., Oldfield, E., Markley, J. L., and Sykes, B. D. (1995) *J. Biomol. NMR 6*, 135−140.
29. Wüthrich, K. (1986) *NMR of Proteins and Nucleic Acids*, Wiley−interscience, New York.
30. Clore, G. M., and Gronenborn, A. M. (1987) *Protein Eng. 1*, 275−288.
31. Wang, Y., Nip, A. M., and Wishart, D. S. (1997) *J. Biomol. NMR 10*, 373−382.
32. Vuister, G. W., and Bax, A. (1993) *J. Am. Chem. Soc. 115*, 7772−7777.
33. Gagne, S. M., Tsuda, S., Li, M. X., Chandra, M., Smille, L. B., and Sykes, B. D. (1994) *Protein Sci. 3*, 1961−1974.
34. Nilges, M., Clore, G. M., and Gronenborn, A. M. (1988) *FEBS Lett. 229*, 317−324.
35. Brunger, A. T. (1992) X-PLOR Version 3.1, *A* System for X-ray Crystallography and NMR, Yale University Press, New Haven, CT.
36. Garrett, D. S., Kuszewski, J., Hancock, T. J., Lodi, P. J., Vuister, G. W., Gronenborn, A. M., and Clore, G. M. (1994) *J. Magn. Reson., Ser. B 104*, 99−103.
37. Kuszewski, J., Gronenborn, A. M., and Clore, G. M. (1995) *J. Magn. Reson., Ser. B 107*, 293−297.
38. Laskowski, R. A., Rullmannn, J. A., MacArthur, M. W., Kaptein, R., and Thornton, J. M. (1996) *J. Biomol. NMR 8*, 477−86.
39. Koradi, R., Billeter, M., and Wuthrich, K. (1996) *J. Mol. Graphics 14*, 51−55.
40. Vriend, D. (1990) *J. Mol. Graphics 8*, 52−56.
41. Williamson, M. P., Kikuchi, J., and Asakura, T. (1995) *J. Mol. Biol. 247*, 541−546.
42. Wishart, D. S., Willard, L., and Sykes, B. D. (1995) VADAR 1.1, University of Alberta, Canada (ftp://redpoll.pharmacy.ualberta.ca).
43. Wishart, D. S., Fortin, S., Woloschuk, D. R., Wong, W., Rosborough, T., Van Domselaar, G. V., Schaeffer, J., and Szafron, D. (1997) *Comput. Appl. Biosci. 13*, 561−562.
44. Dyson, H. J., Jeng, M.-F., Tennant, L. L., Slaby, I., Lindell, M., Cui, D.-S., Kuprin, S., and Holmgren, A. (1997) *Biochemistry 36*, 2622−2636.
45. Wishart, D. S., Sykes, B. D., and Richards, F. M. (1991) *J. Mol. Biol. 222*, 311−322.
46. Wishart, D. S., Sykes, B. D., and Richards, F. M. (1992) *Biochemistry 31*, 1647−1653.
47. Wishart, D. S., Bigam, D. G., Holm, A., Hodges, R. S., and Sykes, B. D. (1995) *J. Biomol. NMR 5*, 67−81.
48. Williamson, M. P. (1990) *Biopolymers 29*, 1423−1431.
49. Wishart, D. S., and Nip, A. M. (1998) *Biochem. Cell Biol. 76*, 1−10.
50. Ikura, M., Kay, L. E., Krinks, M., and Bax, A. (1991) *Biochemistry 30*, 5498−5504.
51. Fimland, G., Jack, R., Jung, G., Nes, I. F., and Nissenmeyer, J. (1998) *Appl. Environ. Microbiol. 64*, 5057−5060.
52. Van Kraaij, C., De Vos, W. M., Siezen, R. J., and Kuipers, O. P. (1999) *Nat. Prod. Rep.* (in press).
53. Bryant, S. H. and Lawrence, C. E. (1993) *Proteins: Struct., Funct., Genet. 16*, 92−112.
54. (a) Ösapay, K., and Case, D. A. (1991) *J. Am. Chem. Soc. 113*, 9436−9444. (b) Ösapay, K., and Case, D. A. (1991) *J. Biomol. NMR 4*, 215−230.
55. Barden, J. A., Cuthbertson, R. M., Wu, J. Z., and Moseley, J. M. (1997) *J. Biol. Chem. 272*, 29572−29578.
56. Kippen, A. D., Arcus, V. L., and Fersht, A. R. (1994) *Biochemistry 33*, 10013−10021.
57. Déméné, H., Dong, C. Z., Ottmann, M., Rouyez, M. C., Jullian, N., Morellet, N., Mely, Y., Darlix, J. L., Fournié-Zaluski, M. C., Saragosti, S., and Roques, B. P. (1994) *Biochemistry 33*, 11707−11716.
58. Volkman, B. F., and Wemmer, D. E. (1997) *Biopolymers 41*, 451−460.
59. Yi, G. S., Choi, B. S., and Kim, H. (1994) *Biophys. J. 66*, 1604−1611.
60. Young, J. K., Hicks, R. P., Wright, G. E., and Morrison, T. G. (1998) *Virology 243*, 21−31.
61. Nelson, J. W., and Kallenbach, N. R. (1989) *Biochemistry 28*, 5256−526l.
62. Merutka, G., and Stellwagen, E. (1989) *Biochemisty 28*, 352−357.
63. Sonnichsen, F. D., Van Eyk, J. E., Hodges, R. S., and Sykes, B. D. (1992) *Biochemistry 31*, 8790−8798.
64. Zhou, N. E., Kay, C. M., Sykes, B. D. and Hodges, R. S. (1993) *Biochemistry 32*, 6190−6197.

BI991351X